Excitation of the $3\,^{1,3}P$ states of Mg by electron impact

G. D. Meneses and C. B. Pagan
Universidade Estadual de Campinas, Instituto de Física "Gleb Wataghin" 13 081 Campinas, São Paulo, Brazil

L. E. Machado
Universidade Federal de São Carlos, 13 560 São Carlos, São Paulo, Brazil
(Received 28 December 1989)

First-order many-body theory was modified to include correlation effects in the target description and used to calculate differential cross sections, coherence, and correlation parameters for the electron-impact excitation of the $3\,^1P$ and $3\,^3P$ states of magnesium at incident energies of 20, 30, 40, 50, and 100 eV. The results are analyzed and compared with available theoretical and experimental results.

I. INTRODUCTION

The study of collision processes involving the Mg atom is of interest to several fields of research, including astrophysics[1] and fundamental collision physics. Among the commonly observed phenomena are those involving inelastic electron scattering by the Mg atom. Early experiments[2–5] on e-Mg inelastic scattering reported results from measurements for excitation functions or absolute integral cross sections for the $3\,^1P \rightarrow 3\,^1S$ resonance line (2852) Å). Previous theoretical work dealt mainly with the computation of multipole strengths[6–10] for the resonance line and for the next few lines. These calculations showed that correlation effects among valence electrons are important for an accurate description of the ground state and some excited states of the atom. As shown by Kim and Bagus,[9,10] these effects can be appropriately taken into account even if one uses a small number of configurations by performing a multiconfigurational Hartree-Fock (MCHF) calculation.

Integral cross sections for inelastic scattering of electrons off magnesium atoms were reported for the $3\,^1S \rightarrow 3\,^1P$ transition by Robb,[11] Van Blerkom,[1] and Fabrikant.[12] Robb used the first-order Born approximation (FBA), and Van Blerkom and Fabrikant both used the close-coupling (CC) approximation. Both CC calculations introduced semiempirical potentials in order to simplify the configuration-interaction (CI) calculation of the bound-state wave functions, which could be a possible cause for the substantial disagreement found among them. The FBA and CC results were obtained for different ranges of the incident electron energies, but a later experiment[13] showed that the FBA integrated cross sections (ICS's) are higher than the observed ones. The above calculations showed that e-Mg scattering can be well described within the LS-coupling scheme.

Absolute elastic and several inelastic differential cross sections (DCS's) were measured by Williams and Trajmar[13] and, more recently, by Teubner and co-workers.[14] They used the technique of energy-loss spectroscopy from the collision of crossed beams of magnesium and electrons with 10-, 20-, and 40-eV impact energies. In a second paper, Fabrikant[15] returned to the e-Mg problem to calculate elastic and $3\,^1S \rightarrow 3\,^1P$ inelastic DCS's for electron-impact energies of 10 and 20 eV in a similar way to what he did before for the ICS's. More recently, Avdonin and Amusia[16] used a many-body technique to calculate inelastic DCS's and the corresponding ICS's for the $3\,^1S \rightarrow 3\,^1P$ and $3\,^1S \rightarrow 3\,^3P$ transitions, for electron-impact energies of 10, 20, and 40 eV. In this latter paper correlation effects among the target electrons were partially introduced through the random-phase approximation with exchange (RPAE), calculated in a simplified way. For the description of the scattering electrons, a single-particle Hartree-Fock model was used, where the incoming (scattered) electron wave function was calculated in the frozen-core potential of the ground (excited) state of the neutral atom. This procedure is known[17] to be equivalent to taking into account, besides the first-order diagram in the scattering electron-atom interaction, an infinite sequence of selected higher-order diagrams. Avdonin and Amusia's values of DCS's are generally in good agreement with the experimental results of Williams and Trajmar[13] and compare better with the experimental results than Fabrikant's corresponding values. However, it appears to us that the partial wave expansion in Avdonin and Amusia's calculation did not converge for the ^1P excitation, as it can be inferred from some of their results which will be discussed later. Recently results from two close-coupling calculations for the $3\,^{1,3}P$ of Mg were reported by McCarthy and co-workers.[18] These calculations are in good agreement with Brunger's experimental data,[14] except for large scattering angles and higher energies.

In the last 15 years, there has been an increasing interest in a new set of collision parameters, namely, the alignment and orientation parameters, which can be measured in electron-photon coincidence experiments. In these experiments, the scattered electron is detected in delayed coincidence with the photon emitted in the atomic deexcitation process. The first such measurements were done by Eminyan *et al.*[19] for the $1\,^1S \rightarrow 2\,^1P$ excitation of helium. Since then, several other experimental groups performed coincidence experiments for He as well

as for other atomic systems. These experiments were the subject of a review article by Andersen, Gallagher, and Hertel.[20] However, only recently have experimental data been published for the coherence parameters of the electron excitation of magnesium.[21]

The present paper refers to the application of the first-order many-body theory (FOMBT), as originally formulated by Csanak, Taylor, and Yaris[22] for inelastic electron-atom scattering, to the e-Mg system. Previous applications of FOMBT to the inelastic scattering of electrons by the rare gases such as He,[23–26] Ne,[27] Ar,[28–29] and Kr (Ref. 30) showed that the theory provides a feasible way of performing accurate well-converged calculations for ICS and DCS, as well as for the alignment and orientation parameters.

We report here results from a FOMBT calculation for the DCS's and of the alignment and orientation parameters for both $3\,^1S \rightarrow 3\,^1P$ and $3\,^1S \rightarrow 3\,^3P$ transitions of magnesium for incident electron energies of 10, 20, 40, 50, and 100 eV. Since this is the first application of FOMBT to a target which is not a rare gas, we also investigated the influence of the target ground state correlation on the collision parameters.

In Sec. II, we present a brief review of the original formulation of the FOMBT along with a discussion on how target state correlation effects are introduced into the present calculation. In Sec. III we discuss some details of the numerical calculation, and in Sec. IV we present the results we obtained for the collision parameters comparing them with both experimental data and theoretical results available in the literature. We shall suggest possible refinements and extensions of the present work and present our conclusions in Sec. V.

II. THEORY

A. The FOMBT

The FOMBT in its original formulation is a nonrelativistic theory that belongs to the general class of distorted-wave approximations (DWA). The T matrix for the excitation of a neutral atom by electron impact is given by[22]

$$T_{nq,op} = \int dx_1 dx_2 [f_q^{(-)}(x_1)]^* f_p^{(+)}(x_2) V_{no}(x_1,x_2) \tag{1}$$

where x_i refers to both spatial $\mathbf{r}_i$ and spin σ_i electron coordinates, p (q) refers to both the momentum $\mathbf{p}$ ($\mathbf{q}$) and the spin component m_{s_1} (m_{s_2}) of the incident (scattered) electron, and $f_k^{(\pm)}(x)$ are the Hartree-Fock continuum orbitals with outgoing (+) and incoming (−) boundary conditions. The indices o and n stand for the quantum numbers of the initial (ground) and final (excited) states of the target, respectively. The transition potential $V_{no}(x_1,x_2)$ is given by

$$V_{no}(x_1,x_2) = \delta(x_1-x_2) \int \frac{dx\, X_n^{\mathrm{RPA}}(x_1,x)}{|\mathbf{r}_1-\mathbf{r}|} - \frac{1}{|\mathbf{r}_1-\mathbf{r}_2|} X_n^{\mathrm{RPA}}(x_2,x_1) \tag{2}$$

where $X_n^{\mathrm{RPA}}(x_1,x_2)$ is the transition density matrix between ground and excited states calculated in the random-phase approximation (RPA). The transition density matrix is defined by the formula

$$X_n(x,x') = \langle \Psi_n | \psi^\dagger(x') \psi(x) | \Psi_0 \rangle \tag{3}$$

where $|\Psi_0\rangle$ and $|\Psi_n\rangle$ are the ground- and excited-state wave vectors of the target, respectively, and $\psi(x), \psi^\dagger(x)$ are the electron field operators in the Schrödinger representation. The transition density matrix can also be given in terms of the wave functions of the ground $\Psi_0(x_1,x_2,\ldots,x_N)$ and excited $\Psi_n(x_1,x_2,..,x_N)$ states in the form

$$X_n(x,x') = N \int \Psi_n^*(x,x_2,\ldots,x_N) \times \Psi_0(x',x_2,\ldots,x_N) dx_2,\ldots,dx_N \tag{4}$$

where N refers to the number of electrons in the target.

In the case of a LS coupled target in a ^1S ground state described by a single Slater determinant (i.e., uncorrelated ground state) the spatial part of the transition density matrix in the Hartree-Fock (HF) model reduces to[25]

$$X_n^{\mathrm{HF}}(\mathbf{r},\mathbf{r}') = \varphi_o(\mathbf{r}) \varphi_n^*(\mathbf{r}') \tag{5}$$

where $\varphi_n(\mathbf{r})$ [$\varphi_o(\mathbf{r})$] is the particle [hole] Hartree-Fock orbital for the active electron in the excited [ground] state of the atom. The differential cross section is given by the formula

$$\sigma = \frac{1}{4\pi^2} \frac{|\mathbf{q}|}{|\mathbf{p}|} \frac{1}{2} \sum_{m_{s_1},m_{s_2}} |T_{nq,op}|^2 . \tag{6}$$

After performing spin summations implicit in Eqs. (1) and (6), we get for the $^1S \rightarrow {}^{1,3}P$ transitions

$$\sigma^{1P}(\theta,M) = \frac{1}{8\pi^2} \frac{|\mathbf{q}|}{|\mathbf{p}|} |2T_{n,o}^D(\theta,M) - T_{n,o}^E(\theta,m)|^2 , \tag{6a}$$

$$\sigma^{3P}(\theta,M) = \frac{3}{8\pi^2} \frac{|\mathbf{q}|}{|\mathbf{p}|} |T_{n,o}^E(\theta,M)|^2 \tag{6b}$$

where θ is the scattering angle and $M=0,\pm1$ refers to the magnetic sublevel of the excited $^{1,3}P$ states. The incident momentum $\mathbf{p}$ was taken in the z-axis direction which was chosen as the quantization direction. The direct and exchange terms of the T matrix are given, respectively, by

$$T_{n,o}^D(\theta,M) = \int f_{\mathbf{p}}^{(+)}(\mathbf{r}) [f_{\mathbf{q}}^{(-)}(\mathbf{r})]^* \frac{1}{|\mathbf{r}-\mathbf{r}'|} \times \varphi_n^*(\mathbf{r}') \varphi_o(\mathbf{r}') d\mathbf{r}\, d\mathbf{r}' , \tag{7a}$$

$$T_{n,o}^E(\theta,M) = \int f_{\mathbf{p}}^{(+)}(\mathbf{r}) [f_{\mathbf{q}}^{(-)}(\mathbf{r}')]^* \frac{1}{|\mathbf{r}-\mathbf{r}'|} \times \varphi_n^*(\mathbf{r}) \varphi_o(\mathbf{r})' d\mathbf{r}\, d\mathbf{r}' . \tag{7b}$$

The electron-photon coincidence parameters λ and χ for the $^1S \rightarrow {}^1P$ transitions are defined by the equations

$$\lambda(\theta) = \frac{\sigma^{1P}(\theta,M=0)}{\sigma^{1P}(\theta,M=0) + 2\sigma^{1P}(\theta,M=1)} , \tag{8a}$$

$$\chi(\theta) = \arg T_{n,o}^{1P}(\theta,M=1) - \arg T_{n,o}^{1P}(\theta,M=0) . \tag{8b}$$

Recently[20] it was found that an alternative set of parameters, named $\langle L_\perp \rangle$ and γ, can be used with certain advantages to interpret electron-atom coincidence experiments leading to LS-coupled excited states. Here $\langle L_\perp \rangle$ is the average angular momentum, perpendicular to the scattering plane, transferred to the motion of atomic electrons and γ is the final state alignment angle of the charge cloud of the target electrons relative to the direction of the incident electron beam. The relation of these new parameters to the previous λ and χ parameters is discussed in the review article by Anderson, Gallagher, and Hertel[20] and is as follows:

$$\langle L_\perp \rangle = -P_3 = -2[\lambda(1-\lambda)]^{1/2}\sin\chi \ , \tag{8c}$$

$$\gamma = \tfrac{1}{2}\arg(P_1 + iP_2) \tag{8d}$$

where the Stokes parameters P_1 and P_2 are related to λ and χ by the equations $P_1 = 2\lambda - 1$, $P_2 = -2[\lambda(1-\lambda)]^{1/2}\cos\chi$. The degree of linear polarization P_l is defined by the equation $P_l = (P_1^2 + P_2^2)^{1/2}$.

B. Application to the Mg target

In previous applications of FOMBT to electron collisions with atoms, the targets were rare gases for which electron correlation effects in the ground state were neglected. In those calculations (3) was simplified by taking $X_n^{\mathrm{RPA}}(\mathbf{r},\mathbf{r}') \approx \varphi_o(\mathbf{r})\varphi_n^*(\mathbf{r}')$ where $\varphi_o(\mathbf{r})$ was obtained self-consistently and $\varphi_n(\mathbf{r})$ was obtained in the field of the frozen-core HF (FCHF) potential of the ion, the so-called V^{N-1} potential. This way of calculating $\varphi_n(\mathbf{r})$ is known[17] to take into account a class of RPA diagrams. In the case of the He target this approximation of $X_n(\mathbf{r},\mathbf{r}')$ produced differences in the DCS's of less than 8% when compared with the first and "exact" FOMBT calculation by Thomas and co-workers.[23,25] This approximation assumes, in effect, an uncorrelated ground state.

For the description of the ground and excited states of the Mg atom, however, electron correlation effects in the ground state are important[6,7] and can be accounted for by using multiconfigurational wave functions.[9,10] One expects that the proper inclusion of electron correlation in FOMBT should require scattering orbitals calculated in the field of the correlated ground state[31] as well as $X_n(\mathbf{r},\mathbf{r}')$ calculated in the multiconfigurational RPA (MCRPA) as proposed, for example, by Yeager and Jorgensen[32] and Dalgaard.[33] Unfortunately, such a complete calculation becomes too lengthy and complex. In order to simplify the calculations, we could use Eq. (4) with multiconfigurational wave functions for Ψ_o and Ψ_n. This corresponds to the level of approximation we previously have used for the uncorrelated rare gases calculations,[25-30] where X_n^{RPA} was substituted by X_n^{HF} [Eq. (5)]. As a first attempt, we actually introduce correlation only in the calculation of the transition potential V_{on}, Eq. (2), via (i) a multiconfigurational (MC) wave function for the ground state in the form

$$|\Psi_0\rangle = a_1|(\mathrm{core})3\bar{s}^2\,{}^1S\rangle + a_2|(\mathrm{core})3\bar{p}^2\,{}^1S\rangle \ , \tag{9}$$

and (ii) a single-configurational excited-state wave function in the form

$$|\Psi_n\rangle = |(\mathrm{core})3\bar{s}3p\,{}^{1,3}P\rangle \tag{10}$$

where the one-electron orbital φ_{3p} is calculated in the frozen-core HF potential constructed from the core + $3\bar{s}$ electron orbitals. It is known that Eq. (9) keeps the most essential contributions to the ground-state description (a similar choice was made by Kim and Bagus[10] and Avdonin and Amusia[16]). The core orbitals φ_{1s}, φ_{2s}, and φ_{3p} in (9) and (10) were those of the single-configuration $|(\mathrm{core})3s^2\,{}^1S\rangle$ HF description of the Mg atomic ground state.

Inserting (9) and (10) in (4) we get for the spatial part of the transition density matrix the formula

$$X_n(\mathbf{r},\mathbf{r}') = a_1\varphi_{3\bar{s}}(\mathbf{r})\varphi_{3p}^*(\mathbf{r}') + \frac{a_2}{\sqrt{3}}\langle 3\bar{p}|3p\rangle\varphi_{3p}(\mathbf{r})\varphi_{3\bar{s}}^*(\mathbf{r}') \ . \tag{11}$$

Each term in (11) has the same form as the simplified X_n^{HF} of Eq. (5), except for a factor proportional to the overlap integral between equivalent electron orbitals which turns up to be not equal to 1 when we use different $3p$ orbitals in (9) and (10). So, the substitution of (11), (4), and (2) in (1) produces the T matrix as a linear combination of two terms each of the form (5), and the formulas for the cross sections, Eqs. (6), (6a), and (6b) then remain valid with T^D and T^E in place of $T_{n,o}^D$ and $T_{n,o}^E$, respectively, the new direct and exchange parts of the T matrix being given by

$$T^{D,E} = a_1 T_{3p,3\bar{s}}^{D,E} + \frac{a_2}{\sqrt{3}}\langle 3\bar{p}|3p\rangle T_{3\bar{s},3p}^{D,E} \ . \tag{12}$$

Note that $a_1 = 1$ and $a_2 = 0$ in (9) result in the simplified LS coupled FOMBT T matrix used in the He calculation.[25] Inclusion of additional configurations mixing in ground and/or excited state would bring nothing significantly new in the formalism but a great deal more of computational work.

III. DETAILS OF THE CALCULATION

A. The target wave functions

We wanted to keep in the model the partial account of higher-order RPA diagrams given by the V^{N-1} potential as mentioned above. This requirement specified our excited electron orbital φ_{3p} in (9). We used the optical oscillator strength (OS) for the $3\,{}^1S \rightarrow 3\,{}^1P$ transition as a criterium to select from among the various possible ways of calculating $|\Psi_0\rangle$. For comparison we show in Table I values for the OS of that transition collected in the literature from several authors. The list is not complete and all values there refer to the length form of the OS. We can see that in order to achieve good OS values, CI procedures followed by Zare,[7] Robb,[11] and Norcross[34] require the inclusion of a large number of configurations in the description of both ground and excited states. For numerical reasons we would like to avoid this. On the other hand, Kim and Bagus[10] obtained a reasonably good

TABLE I. Oscillator strength for the $3\,^1S \rightarrow 3\,^1P$ transition of Mg, length form.

Experiment	Robb[a]	Zare[b]	Norcross[c]	Kim and Bagus[d]	Present
1.810±0.005[e] 1.83±0.08[f]	1.814	1.72	1.835	1.71	1.83

[a]CI calculation with 20 configurations in the ground state and 23 in the excited state (Ref. 11).
[b]CI calculation (local exchange) with eight configurations in the ground state and nine in the excited state (Ref. 7).
[c]CI calculation with six configurations in the ground state and four in the excited state (Ref. 34).
[d]MCHF calculation with two configurations in the ground state and two in the excited state (Refs. 9 and 10).
[e]Experimental values of Smith and Gallagher (Ref. 2).
[f]Experimental value of Liljeby *et al.* (Ref. 36).

OS value with just one additional configuration in the ground-state wave function using the multiconfigurational (MCHF) scheme of Froese-Fischer.[35] In this scheme the φ_{3s} electron orbital is relaxed by allowing it to interact with the φ_{3p} one. In fact, using the relaxed $\varphi_{3\bar{s}}$ orbital along with the φ_{3p} excited electron orbital calculated in the FCHF scheme, we got for the OS the value 1.828, in excellent agreement with the experimental value.[36] So we followed the MCHF procedure to calculate $|\Psi_o\rangle$ in Eq. (8). The bound electron orbitals were all obtained from the Froese-Fischer computer program. The obtained mixing coefficients were $a_1=0.961\,480\,3$ and $a_2=0.274\,873\,81$ and the ground-state energy was $E_o^{\rm MC}=-0.646\,068\,8$ a.u. against the value $E_o=-0.614\,636\,4$ a.u. given by the single-configuration HF calculation. Throughout this work we used the experimental values[13] for the excitation energies $\omega(^1P)=0.159\,775$ a.u. and $\omega(^3P)=0.099\,688$ a.u.

B. The scattering orbitals

The continuum orbitals $f_{\rm p}^{(+)}(\mathbf{r})$ and $f_{\rm q}^{(-)}(\mathbf{r})$ in Eqs. 7(a) and 7(b) were partial-wave analyzed, leading to the radial components $u_{l,k}(r)$ of well-defined linear (k) and angular (l) momenta. We used a modified version of the linear algebraic static exchange code of Collins and Schneider[37] to calculate those radial functions in the field of the uncorrelated Mg ground state. The differential equation for the distorted partial waves was integrated in a radial grid up to 25 a.u. and then the solutions were fit to the exact asymptotic wave functions. We obtained phase shifts for l varying from 0 to $l_D=7$ for $E_i=10$ eV and from 0 to $l_D=22$ for $E_i=100$ eV.

C. The T-matrix expansion

The T matrices in Eqs. 7(a) and 7(b) are then written as partial wave expansions in the form

$$T_{n,o}^{D,E}(\theta,M)=\sum_l T_l^{D,E}(M)P_l^M(\cos\theta)\ .$$

In the numerical calculation of these expressions we must truncate the sums at a finite $l=l_D$. However, it is known that the direct part $T_{n,o}^D(\theta,M)$ converges slowly. In order to account for the $l_D<l<\infty$ contributions to $T_{n,o}^D(\theta,M)$, we used the technique[38] of summing to and subtracting from it the T matrix calculated in the first-order Born approximation. Also, the direct part of the T matrix involves a two-electron radial integration ranging to infinity. We used an accurate numerical integration technique to calculate it from $r=0$ to $r=R_1=600$ a.u. and performed analytically the integration for $R_1<r<\infty$ using the asymptotic form of the integrand, a procedure first adopted by Madison and Shelton.[39]

IV. RESULTS AND DISCUSSION

In Fig. 1 we show the Mg phase shifts $\delta_l(E)$ for the partial waves s,p,d for energies $E\leq 100$ eV. At 10, 20, and 40 eV our values agree with the ones published by Avdonin and Amusia.[16] For a given energy the phase shifts decrease very slowly with the increase of the angular momentum l, thus posing the need of inclusion of many distorted waves in the T-matrix summation.

For comparison and analysis we performed for energies of 10, 20, and 40 eV the calculations of cross sections and coherence and correlation parameters using both the single-configuration (SC) $[(3s)^2]$ and double-configuration (DC) $[(3\bar{s})^2$ and $(3p)^2]$ representations of the Mg ground state in Eq. (9). Tables II and III display our SC results for the excitation of the $3\,^1P$ and $3\,^3P$ states of Mg at in-

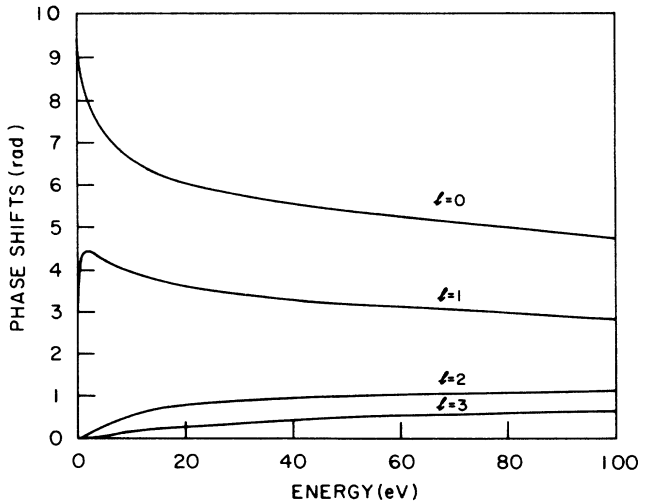

FIG. 1. Present results for the Mg phase shifts δ_l as a function of the electron energy.

TABLE II. Present results for differential cross sections (in cm^2) for the $3\,^1S \rightarrow 3\,^1P$ transition of Mg, single configuration calculation. $[-\chi]$ denotes $\times 10^{-\chi}$.

θ	$\sigma(\theta,E)$ (cm^2/sr)					
(deg)	$E=10$ eV	$E=20$ eV	$E=30$ eV	$E=40$ eV	$E=50$ eV	$E=100$ eV
0	7.08[−15]	2.77[−14]	4.92[−14]	7.08[−14]	9.26[−14]	2.02[−13]
10	4.53[−15]	6.99[−15]	5.47[−15]	4.03[−15]	3.00[−15]	8.86[−16]
20	1.73[−15]	1.11[−15]	5.26[−16]	2.69[−16]	1.49[−16]	2.17[−17]
30	5.96[−16]	2.20[−16]	8.48[−17]	4.33[−17]	2.62[−17]	6.44[−18]
40	2.47[−16]	8.25[−17]	3.54[−17]	1.89[−17]	1.11[−17]	2.34[−18]
50	1.45[−16]	4.53[−17]	1.77[−17]	8.64[−18]	5.09[−18]	1.31[−18]
60	1.05[−16]	2.52[−17]	9.98[−18]	5.69[−18]	4.12[−18]	1.10[−18]
70	7.63[−17]	1.52[−17]	8.74[−18]	6.25[−18]	4.81[−18]	9.65[−19]
80	5.25[−17]	1.21[−17]	9.88[−18]	7.20[−18]	5.18[−18]	7.07[−19]
90	3.40[−17]	1.20[−17]	1.05[−17]	7.04[−18]	4.54[−18]	3.43[−19]
100	2.21[−17]	1.22[−17]	9.70[−18]	5.69[−18]	3.23[−18]	6.33[−20]
110	1.64[−17]	1.13[−17]	7.71[−18]	4.00[−18]	2.10[−18]	1.63[−19]
120	1.56[−17]	9.51[−18]	5.71[−18]	3.22[−18]	2.22[−18]	9.25[−19]
130	1.77[−17]	7.20[−18]	8.49[−18]	4.34[−18]	4.29[−18]	2.50[−18]
140	2.10[−17]	4.99[−18]	5.88[−18]	7.65[−18]	8.38[−18]	4.80[−18]
150	2.41[−17]	3.36[−18]	8.49[−18]	1.25[−17]	1.38[−17]	7.48[−18]
160	2.62[−17]	2.40[−18]	1.18[−17]	1.77[−17]	1.93[−17]	1.00[−17]
170	2.73[−17]	1.94[−18]	1.45[−17]	2.17[−17]	2.33[−17]	1.18[−17]
180	2.76[−17]	1.82[−18]	1.55[−17]	2.32[−17]	2.48[−17]	1.25[−17]

cident energies of 10, 20, 30, 40, 50, and 100 eV. Tables IV and V show our SC results for the χ and λ parameters, respectively, for the $3\,^1S \rightarrow 3\,^1P$ transition and energies of 10, 20, 30, 40, 50, and 100 eV.

The cross sections. In the top of Figs. 2 and 3 we present our theoretical SC and DC results for the DCS at $E_i = 10$, 20, and 40 eV along with the experimental results of Brunger and co-workers and the ones of Williams and Trajmar[13] for the $3\,^1P$ and $3\,^3P$ excitations. For $E_i = 30$, 50, and 100 eV there is no experimental or other theoretical data to compare with. For reference, we include in these cases the FBA cross sections.

We observe in these figures that the structures of the DC curves are essentially the same as the corresponding SC ones. For the $3\,^1P$ case at all energies the inclusion of the $(3p)^2$ configuration produced a better overall qualitative result, leading to a better description of the first minimum intensity at intermediate scattering angles. Equation (12) shows that since $\varphi_{3\bar{s}}$ and φ_{3s} are not too different (and $a_1 \approx 0.96$) the first term gives a contribution to the DC DCS which is about 10% less than the SC DCS. In fact, the second term of Eq. (12) was the one

TABLE III. Same as Table II, except for the $3\,^1S \rightarrow 3\,^3P$ transition. $[-\chi]$ denotes $\times 10^{-\chi}$.

θ	$\sigma(\theta,E)$ (cm^2/sr)					
(deg)	$E=10$ eV	$E=20$ eV	$E=30$ eV	$E=40$ eV	$E=50$ eV	$E=100$ eV
0	1.18[−16]	1.89[−17]	5.22[−18]	2.04[−18]	1.10[−18]	1.27[−19]
10	1.25[−16]	2.53[−17]	9.78[−18]	5.45[−18]	3.66[−18]	1.10[−18]
20	1.39[−16]	3.25[−17]	1.25[−17]	6.17[−18]	3.45[−18]	3.56[−19]
30	1.42[−16]	2.83[−17]	7.88[−18]	2.69[−18]	1.04[−18]	2.11[−20]
40	1.26[−16]	1.81[−17]	3.26[−18]	7.04[−19]	1.80[−19]	1.39[−20]
50	9.87[−17]	9.62[−18]	1.19[−18]	2.15[−19]	7.46[−20]	1.08[−20]
60	7.02[−17]	4.63[−18]	4.66[−19]	1.01[−19]	4.87[−20]	4.94[−21]
70	4.66[−17]	1.98[−18]	1.83[−19]	5.78[−20]	3.34[−20]	2.64[−21]
80	2.93[−17]	7.34[−19]	1.55[−19]	8.61[−20]	4.69[−20]	1.84[−21]
90	1.76[−17]	4.48[−19]	3.14[−19]	1.59[−19]	7.11[−20]	1.05[−21]
100	1.02[−17]	7.54[−19]	5.16[−19]	2.13[−19]	7.96[−20]	2.36[−22]
110	5.98[−18]	1.23[−18]	6.23[−19]	2.14[−19]	6.75[−20]	3.20[−22]
120	4.32[−18]	1.53[−18]	5.81[−19]	1.72[−19]	5.05[−20]	2.37[−21]
130	4.65[−18]	1.51[−18]	4.44[−19]	1.37[−19]	5.49[−20]	7.02[−21]
140	6.32[−18]	1.25[−18]	3.13[−19]	1.52[−19]	9.69[−20]	1.41[−20]
150	8.67[−18]	8.89[−19]	2.56[−19]	2.31[−19]	1.74[−19]	2.25[−20]
160	1.11[−17]	5.77[−19]	2.84[−19]	1.48[−19]	2.65[−19]	3.04[−20]
170	1.29[−17]	3.93[−19]	3.44[−19]	4.50[−19]	3.38[−19]	3.63[−20]
180	1.36[−17]	3.36[−19]	3.74[−19]	4.89[−19]	3.67[−19]	3.81[−20]

TABLE IV. SC results for the χ parameter for the $3\,^1S \rightarrow 3\,^1P$ transition of Mg.

Angle (deg)	χ parameter (rad) 10 eV	20 eV	30 eV	40 eV	50 eV	100 eV
10	−0.314 20	−0.289 56	−0.350 99	−0.432 02	−0.517 69	−0.977 06
20	−0.609 73	−0.841 97	−1.094 30	−1.304 30	−1.442 50	−1.451 10
30	−1.078 60	−1.196 40	−1.214 30	−1.183 60	−1.139 60	−0.939 46
40	−1.425 00	−0.927 28	−0.890 15	−1.046 50	5.050 80	4.970 50
50	−1.357 90	−0.805 10	−1.236 20	4.527 90	4.136 80	2.346 80
60	−1.043 30	−1.170 70	3.946 40	3.312 60	2.897 40	1.688 60
70	−0.934 26	4.074 30	2.784 50	2.315 80	1.993 70	1.359 20
80	−1.013 50	2.895 80	2.067 30	1.670 40	1.446 50	1.111 80
90	5.082 80	2.299 40	1.555 00	1.201 10	1.035 30	0.917 73
100	4.743 40	1.907 50	1.076 20	0.724 46	0.549 10	−1.961 60
110	4.035 00	1.535 40	0.445 04	0.122 74	−0.047 87	0.505 88
120	3.247 00	0.438 19	−0.179 32	−0.138 94	−0.006 95	0.571 41
130	2.901 50	−0.989 37	−0.246 99	0.143 69	0.323 15	0.536 40
140	2.7685	−1.119 00	0.061 27	0.384 97	0.456 39	0.503 31
150	2.712 20	−0.936 20	0.309 30	0.478 95	0.495 33	0.478 13
160	2.686 40	−0.562 51	0.424 70	0.510 68	0.504 64	0.460 87
170	2.674 30	−0.243 54	0.470 20	0.521 50	0.505 56	0.450 60

that reinforced the structure of maxima and minima of the DCS, the final result being that the DCS curves were lowered for the 20 and 40 eV, and the minima showed up more clearly. We can see also in Figs. 2(a), 2(b), and 2(d) that ground-state correlation becomes less important with increasing energies for the $1P$ case, but the same is not true for the ^3P case shown in Figs. 3(a), 3(b), and 3(d).

Comparing the SC and DC DCS's with the experimental data, we can see that the frontal peak of intensity, characteristic of optically allowed transitions, is well reproduced by the FOMBT, although it resulted in both cases a bit overestimated at $E_i = 10$ and 20 eV. This can be explained by the fact that Mg has a polarizability of $\alpha_o = 75.0$ (Ref. 40) and probably at lower energies the continuum electron is slow enough to feel the long-range polarization potential of the target. Nevertheless, this effect is no more felt at $E_i = 40$ eV and above. The theoretical results of Avdonin and Amusia[16] shown in their Fig. 2 do not present this peak in the forward direction. They report the inclusion of at most six partial waves in their calculation and speculate that this may be the cause of the failing of the theory at small angles. We have calculated the DCS for $E_i = 40$ eV including only the first six distorted partial waves and obtained a forward differential cross section $\sigma(\theta = 0°)$ two orders of magnitude smaller than the full calculation. This shows that Avdonin and Amusia's assumption was right and once more evidences the need for the inclusion of a large number of terms in the direct T-matrix summation.

At intermediate scattering angles the DC curves show structures in excellent qualitative agreement with the recent measurements of Brunger and co-workers.[14] Quanti-

TABLE V. SC results for the λ parameter for the $3\,^1S \rightarrow 3\,^1P$ transition of Mg.

Angle (deg)	λ parameter 10 eV	20 eV	30 eV	40 eV	50 eV	100 eV
10	0.750	0.370	0.199	0.123	0.086	0.034
20	0.478	0.241	0.191	0.195	0.223	0.520
30	0.445	0.458	0.521	0.575	0.606	0.745
40	0.634	0.640	0.543	0.521	0.560	0.930
50	0.822	0.507	0.342	0.411	0.592	0.974
60	0.849	0.279	0.239	0.483	0.701	0.833
70	0.784	0.140	0.415	0.631	0.733	0.745
80	0.669	0.286	0.629	0.720	0.757	0.756
90	0.505	0.576	0.767	0.790	0.805	0.861
100	0.304	0.804	0.860	0.848	0.853	0.947
110	0.177	0.940	0.905	0.844	0.797	0.222
120	0.263	0.992	0.852	0.695	0.608	0.578
130	0.475	0.955	0.703	0.615	0.644	0.735
140	6.671	0.833	0.665	0.721	0.770	0.836
150	0.816	0.695	0.777	0.843	0.873	0.909
160	0.916	0.694	0.898	0.931	0.945	0.960
170	0.978	0.878	0.975	0.983	0.986	0.990

tative deviations (by a factor of ~4 at 10 eV and of ~7 at 40 eV) are observed when one compares the present DC curves to the experimental data at intermediate scattering angles. Similar behavior, although showing smaller quantitative deviations, is observed in the more elaborated five-state CC calculation by McCarthy and Mitroy.[18] Such deviations can be partially accounted for by the fact that we have calculated the continuum wave functions in the field of the uncorrelated ground state of the atom. For the $3\,^1P$ state and small scattering angles, this is a reasonable procedure, because the calculation of the cross section in this region is dominated by the direct part of the T matrix. For a good description of the latter an infinite number of partial waves has to be considered. In this case the low-l partial wave components, for which distortion does matter, do not significantly contribute to the final result. However, for intermediate angles in the ^1P excitation, where the direct and exchange parts of the T matrix become competitive, and for all angles in the ^3P excitation, which is a pure exchange process, the T matrix is dominated by the low-l distorted partial waves and therefore the use of the correct first-order distortion potential certainly will make a difference. Previous FOMBT DCS's calculated for the rare gases,[23–30] for which electron correlation in the ground state is not important show also some discrepancies when compared to experimental results at large angles ($\theta > 120°$) for ^1P transitions. For the ^3P transitions the Mg FOMBT DCS's are nearly of the same quality as those obtained for the rare gases and are in good agreement with recently published

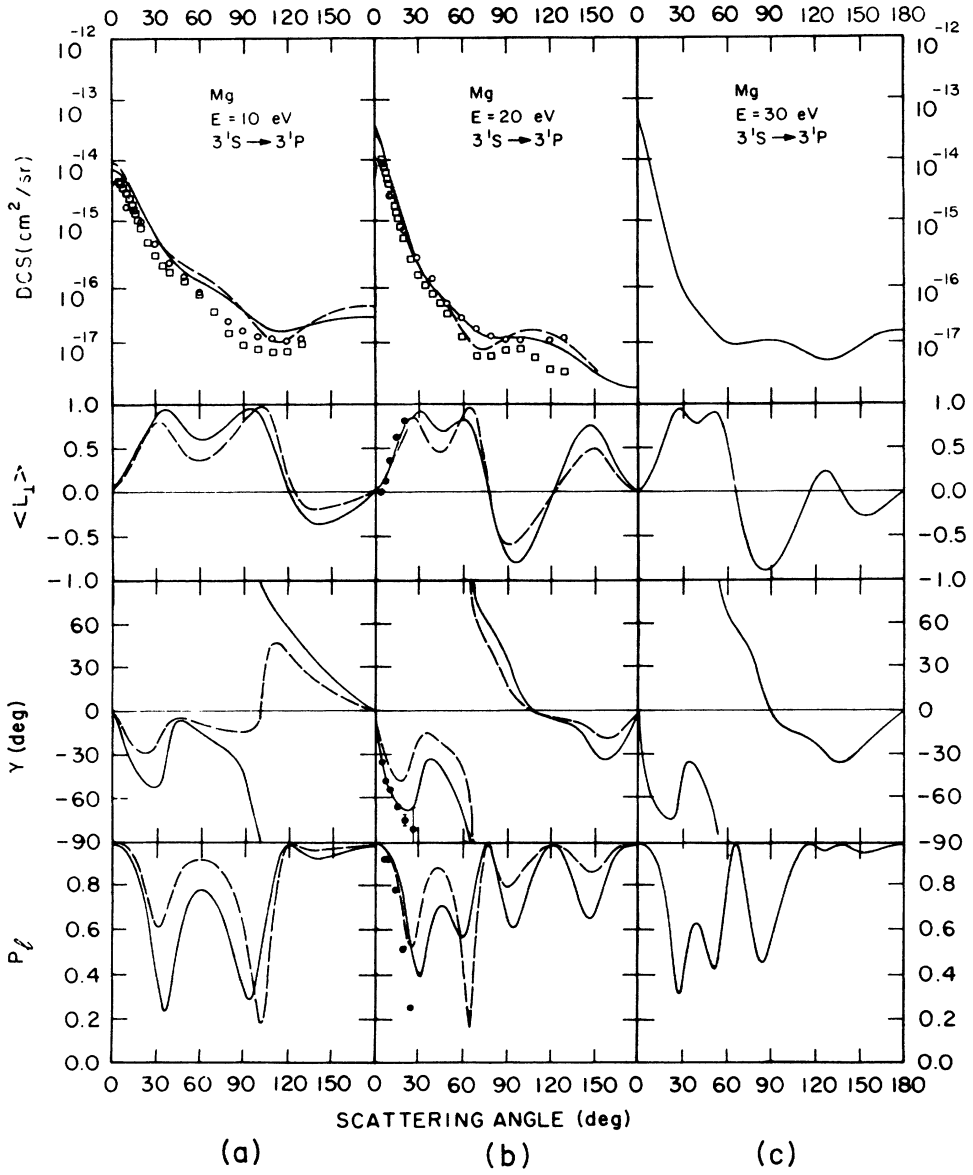

FIG. 2. DCS, $\langle L_\perp \rangle$, γ, and P_l for the $3^1S \rightarrow 3\,^1P$ transition of Mg. (a) $E = 10$ eV; (b) $E = 20$ eV; (c) $E = 30$ eV; (d) $E = 40$ eV; (e) $E = 50$ eV; (f) $E = 100$ eV. ——, present results, SC; — — —, present results, DC; ○, experimental results (Ref. 14); ●, experimental results (Ref. 21); □, experimental results of Williams and Trajmar (Ref. 13); —·—·—·, first Born approximation.

experimental results.[14] All this leads to the conclusion that, as far as the DCS calculation is concerned, the inclusion of additional configurations in the description of the target states may be of less importance than the inclusion of the several second order effects. Even the $|3s3p\rangle$ configuration (that appears in the description of the $3\,^1P$ excited state with a mixing coefficient $a=0.219$, see Table II of Kim and Bagus[10]) will give a small quantitative contribution to the DCS, because its final contribution will come out multiplied by a factor of ≈ 0.06.

The coherence and correlation parameters. The analysis of our results for the coherence and correlation parameters is severely limited by the lack of experimental or other theoretical results to compare with. The very recent results of Brunger *et al.*[21] for the λ and $\cos\chi$ parameters are, to our knowledge, the only experimental results for the excitation of the $3\,^1P$ level of Mg. On the theoretical side there is a recent publication by Mitroy and McCarthy[18] that gives the Stokes parameters for the same transition at 20 and 40 eV. At the present time, there are no available results for the $3\,^3P$ level. In Figs. 2 and 3 we show our results for the $\langle L_\perp \rangle$ and γ parameters, along with the corresponding values extracted from the experiment.[21] For every case where both SC and DC calculations were done, we can observe that inclusion of target correlation does not alter the general structure of the curves. For both parameters the use of the correlated DC wave function for the target led to only slightly different maxima and minima angular positions, but the peak intensities are affected up to a factor of 1.8. It is interesting to note that the isolated discontinuity of the alignment angle γ present in certain energies is smoothed out in the DC calculation at $E=10$ and 40 eV in the optically allowed transition. It should be useful, at this point,

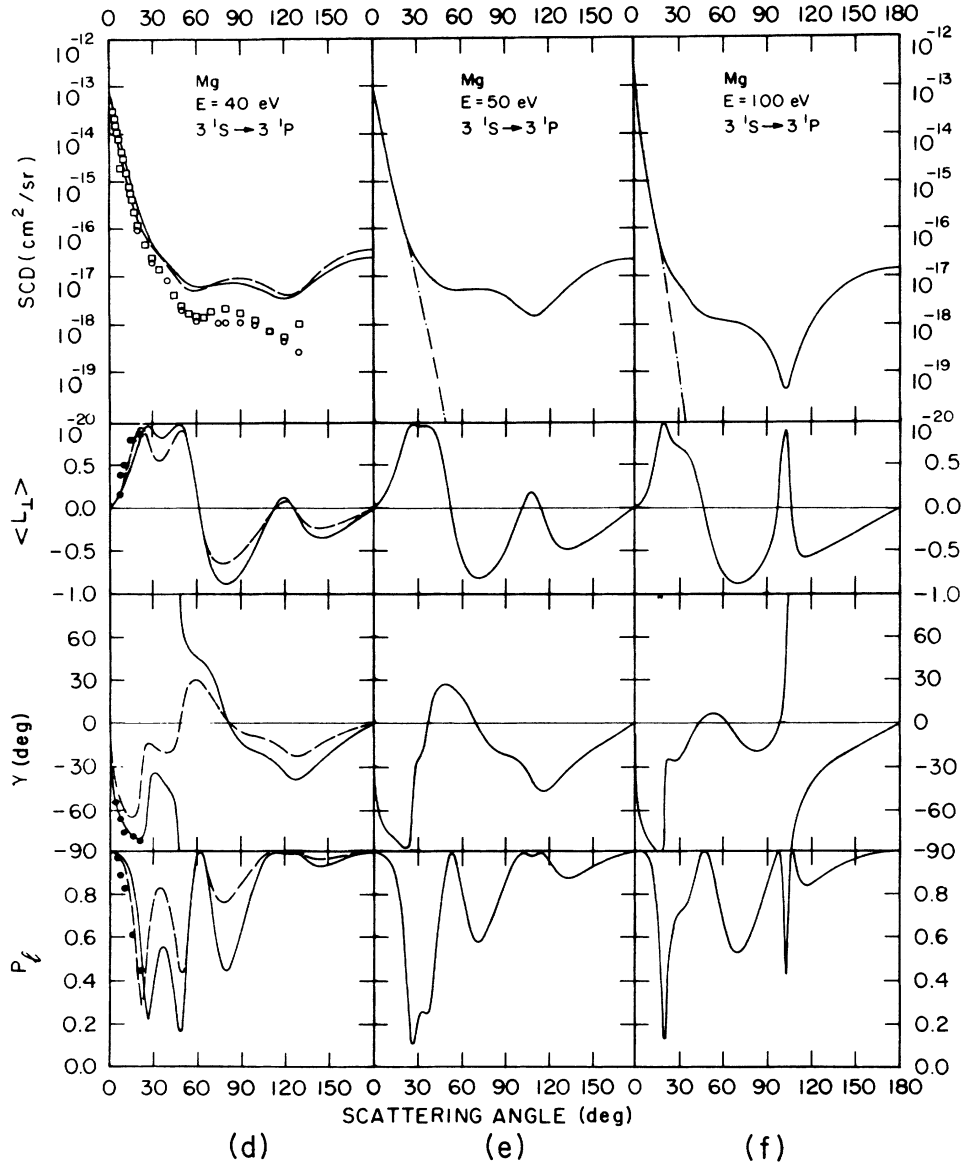

FIG. 2. (*Continued*).

recall that the γ parameter is defined modulo π.

In all cases where experimental results are available [Figs. 2(b) and 2(d)], agreement is observed between theory and experiment. Our DC values for $\langle L_\perp \rangle$ are closer to the experimental results than the corresponding values from the SC calculation. For the γ parameter, contrarily, our SC values are closer to the experimental ones. In fact, the present results for $\langle L_\perp \rangle$, γ, and P_l compare with Brunger's experimental data as well as the more elaborate CC results.[18]

The results for the DCS, $\langle L_\perp \rangle$, and γ parameters for both $3\,^1S \rightarrow 3\,^1P$ and $3\,^1S \rightarrow 3\,^3P$ transitions can be directly compared to the corresponding results for the $1\,^1S \rightarrow 2\,^1P$ and $1\,^1S \rightarrow 2\,^3P$ excitations of He, by using appropriate energy ratios.[41] In fact, for the $3\,^1S \rightarrow 3\,^1P$ transition of Mg, several characteristic features present in the corresponding transition of He can be observed. We can observe, for example, that $\langle L_\perp \rangle$ has only one zero (occurring at $\theta = 125°$) for low incident energy ($E_o = 10$ eV) and two or more zeros for higher incident energies. This behavior is also observed in He, when one compares the corresponding curves at incident energies of 50 and 100 eV or higher.[20] Also, it can be observed in Figs. 2(a)–2(f) that the angular position of the first zero of $\langle L_\perp \rangle$ goes to smaller angles for increasing incident energies, as observed in the He cases.[20] Besides that, as in the He case, more and more oscillations in the $\langle L_\perp \rangle$ curves can be seen as the incident energy goes up. This is due to interference effect as discused by Madison, Csanak, and Cartwright[42] for the He case. The larger number of oscillations in the Mg target is probably due to the fact that here a larger number of phases are different from zero and thus a more complex interference pattern arises. One should note, however, that for the triplet transitions no regular similarities can be found between the He and Mg cases.

It is well established now that $\langle L_\perp \rangle$ is positive for small scattering angles for the rare gases, where the initial state is an $s^2\,^1S$ or a $p^6\,^1S$ state and the excited state is an $sp\,^1P$ or a $p^5s\,^1P$ state, respectively. The first term of

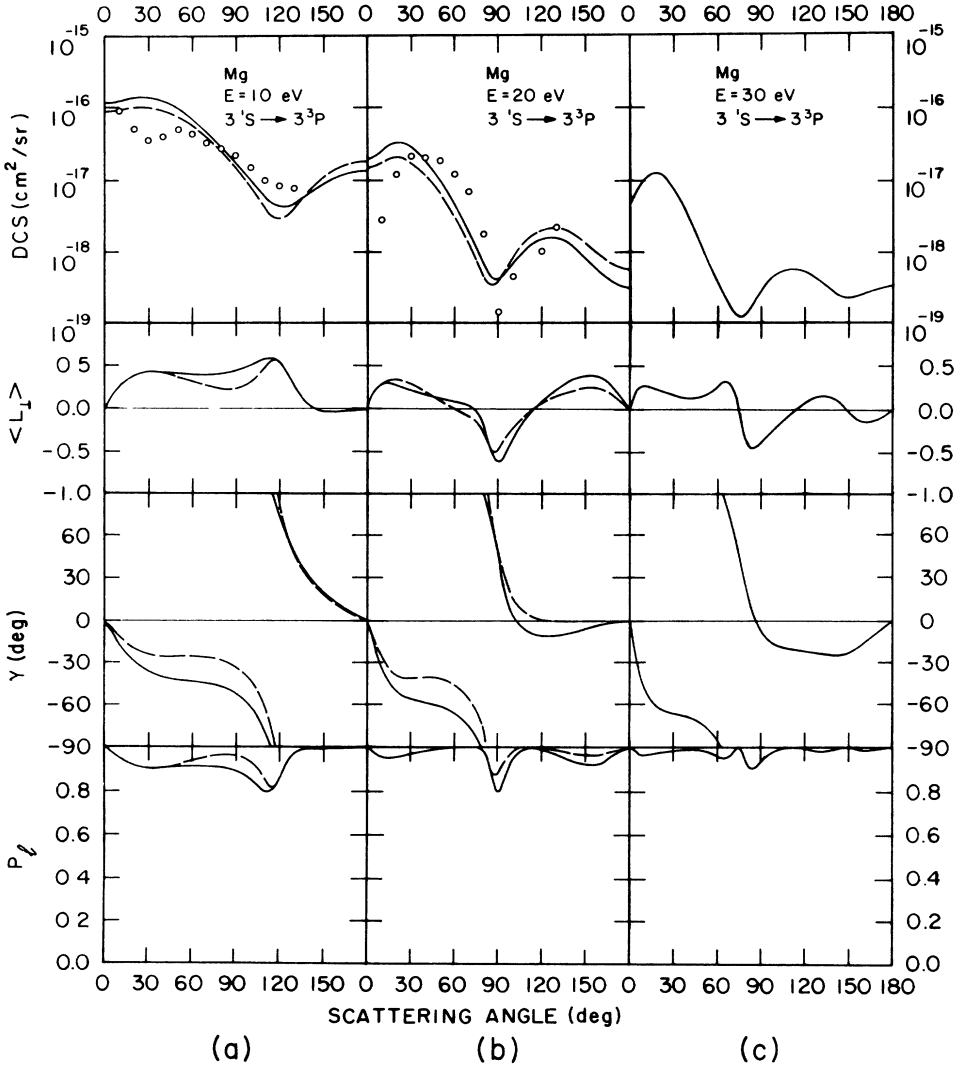

FIG. 3. Same as Fig. 2 for the $3\,^1S \rightarrow 3\,^3P$ transition of Mg.

the T matrix in Eq. (12) is identical, from the angular-momentum-analysis point of view, to the helium T matrix and, as expected, the signal behavior of $\sin\chi$ in the SC calculation is similar to the one obtained previously for He. The second term, however, is *not* the same as the T matrix for the heavier rare gases (Ar, for example). This second term involves the coupling of one p electron and one s electron and for heavy rare gases the coupling involves the electron configuration p^5s or, equivalently, the coupling of one p hole and one s electron. This means[43] that the excitation of an atom from an initial previously prepared $p^2\,^1S$ state to a final $ps\,^1P$ state would produce negative values for the average transferred angular momentum $\langle L_\perp \rangle$ at small scattering angles.

As a final observation, we can mention the existing relationship for the singlet transition of Mg, between the maxima and minima of the DCS and the zeros of the γ and $\langle L_\perp \rangle$ parameters, respectively. In fact, observation of Fig. 2 shows that for the $3\,^1S \rightarrow 3\,^1P$ transition of Mg the angular positions of the first minimum of the DCS and of the first zero of $\langle L_\perp \rangle$ are nearly coincident. The same observation can be made for the positions of the local maximum occurring in the DCS curves (except at $E_o = 10$ eV) and of the zeros in the γ parameter. These relations are similar to those observed in Kessler effect.[44] However, the explanation for such relations cannot be given in terms of spin-orbit interaction, which is negligible in our case and was not included in the calculation.

V. CONCLUSIONS

In this work we presented a FOMBT calculation for the DCS and alignment and orientation parameters for the $3\,^1S \rightarrow 3\,^1P$ and $3\,^1S \rightarrow 3\,^3P$ excitation of the Mg atom. The ground state of the target was described by either single-configurational Hartree-Fock (SCHF) or MCHF approximations, and we compared these two approaches in order to get an insight on the relative importance of

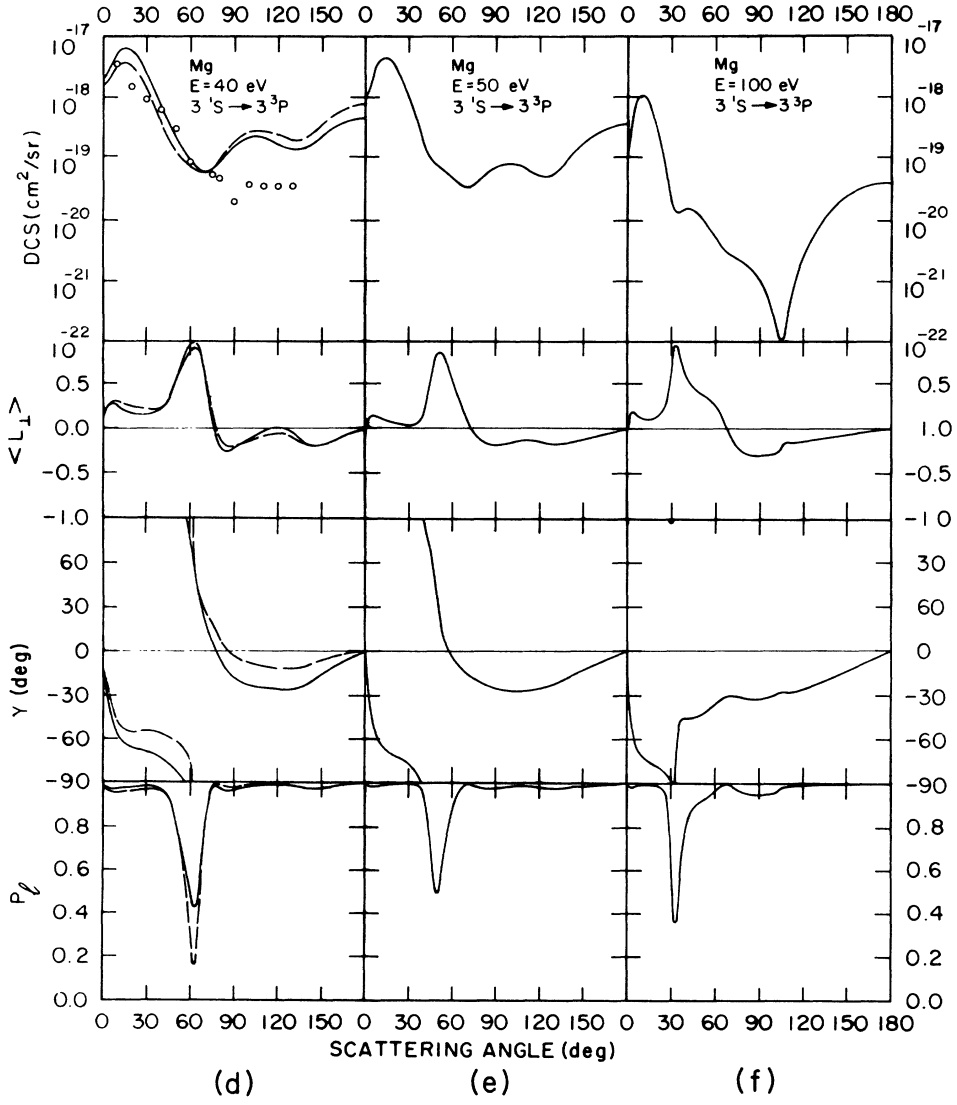

FIG. 3. (*Continued*).

the target electron correlation. We have found that, in general, this correlation affects only slightly the calculated absolute values of the DCS. However, the MCHF calculation in most cases leads to a better defined structure of maxima and minima in the DCS curves. From the comparison among present and previous FOMBT results for the rare gases, we conclude that in order to improve quantitatively the cross-section results for intermediate and large scattering angles, we should possibly first consider the scattering orbitals in the field of correlated target,[31] and second include higher-order terms in the many-body expansion of the two-particle effective potential.[22] In respect to the alignment and orientation parameters, the lack of experimental results drastically reduces the possibility of comparison. However, for small scattering angles, the data from Brunger[21] for both the $\langle L_\perp \rangle$ and γ parameters are fairly reproduced by our calculation.

ACKNOWLEDGMENTS

The authors gratefully acknowledge the support of Conselho Nacional de Desenvolvimento Científico e Tecnológico (CNPq-Brazil). We also thank Dr. G. Csanak and Dr. D. C. Cartwright for valuable discussions and L. A. Collins and B. I. Schneider for the use of their linear algebraic program.

[1]J. K. Van Blerkom, J. Phys. B **3**, 932 (1970).
[2]W. W. Smith and A. Gallagher, Phys. Rev. **145**, 26 (1966).
[3]F. Karstensen and H. Köster, Astron. Astrophys. **13**, 116 (1971).
[4]I. S. Aleksakhin, I. P. Zapesochnyi, I. I. Garza, and V. P. Staredub, Opt. Spectrosk. **34**, 1053 (1973) [Opt. Spectrosc. (USSR) **34**, 611 (1973)].
[5]D. Leep and A. Gallagher, Phys. Rev. A **13**, 148 (1976).
[6]R. N. Zare, J. Chem. Phys. **45**, 1966 (1966).
[7]R. N. Zare, J. Chem. Phys. **47**, 3561 (1967).
[8]A. W. Weiss, J. Chem. Phys. **47**, 3573 (1967).
[9]Y. K. Kim and P. S. Bagus, J. Phys. B **5**, L193 (1972).
[10]Y. K. Kim and P. S. Bagus, Phys. Rev. A **8**, 1739 (1973).
[11]W. D. Robb, J. Phys. B **7**, 1006 (1974); in *Abstracts of Contributed Papers of the Ninth International Conference on the Physics of Electronic and Atomic Collisions, Seattle, 1975,* edited by J. S. Risley and R. Geballe (University of Washington, Seattle, 1975), pp. 1113 and 1114.
[12]I. I. Fabrikant, J. Phys. B **7**, 91 (1974).
[13]W. Williams and S. Trajmar, J. Phys. B **11**, 2021 (1978).
[14]M. J. Brunger, J. R. Riley, R. E. Scholten, and P. J. O. Teubner, J. Phys. B **21**, 1639 (1988); R. K. Houghton, G. F. Shen, M. J. Brunger, and P. J. O. Teubner (unpublished).
[15]I. I. Fabrikant, J. Phys. B **13**, 603 (1980).
[16]N. B. Avdonin and M. Ya. Amusia, J. Tech. Phys. **53**, 341 (1983).
[17]M. Ya. Amusia, N. A. Cherepkov, and L. V. Chernysheva, Zh. Eksp. Teor. Fiz. **60**, 160 (1971) [Sov. Phys.-JETP **33**, 90 (1971)].
[18]J. M. Mitroy and I. E. McCarthy, J. Phys. B **23**, 641 (1989); I. E. McCarthy, K. Ratnavelu, and Y. Zhou, *ibid.* **22**, 2597 (1989).
[19]M. Eminyan, K. B. MacAdam, J. Slevin, and H. Kleinpoppen, Phys. Rev. Lett. **31**, 576 (1973).
[20]N. Andersen, J. W. Gallagher and I. V. Hertel, Phys. Rep. **165**, 1 (1988); in *Invited Papers of the Fourteenth International Conference on the Physics of Electronic and Atomic Collisions, Palo Alto, 1985,* edited by M. J. Coggiola, D. L. Huestis, and R. P. Saxon (North-Holland, Amsterdam, 1986).
[21]M. J. Brunger, J. L. Riley, R. E. Scholten, and P. J. O. Teubner, J. Phys. B **22**, 1431 (1989).
[22]G. Csanak, H. S. Taylor, and R. Yaris, Adv. At. Mol. Phys. **7**, 287 (1971); Phys. Rev. A **3**, 1322 (1971).
[23]L. D. Thomas, G. Csanak, H. S. Taylor, and B. S. Yarlagadda, J. Phys. B **7**, 1719 (1974).
[24]A. Chutjian and L. D. Thomas, Phys. Rev. A **11**, 1583 (1975).
[25]G. D. Meneses, N. T. Padial, and G. Csanak, J. Phys. B **11**, L237 (1978).
[26]G. D. Meneses and G. Csanak, Z. Phys. D **8**, 219 (1988).
[27]L. E. Machado, E. P. Leal, and G. Csanak, J. Phys. B **15**, 1773 (1982); Phys. Rev. A **29**, 1811 (1984).
[28]N. T. Padial, G. D. Meneses, F. J. da Paixão, G. Csanak, and D. C. Cartwright, Phys. Rev. A **23**, 2194 (1981).
[29]F. J. da Paixão, N. T. Padial, and G. Csanak, Phys. Rev. A **30**, 1697 (1984).
[30]G. D. Meneses, F. J. da Paixão, and N. T. Padial, Phys. Rev. A **32**, 156 (1985).
[31]J. P. Swanson and L. Armstrong, Jr., Phys. Rev. A **15**, 661 (1977); *ibid.* **16**, 1117 (1977).
[32]D. L. Yeager and P. Jørgensen, Chem. Phys. Lett. **65**, 77 (1987).
[33]E. Dalgaard, J. Chem. Phys. **72**, 816 (1980).
[34]D. Norcross, as referred to by W. D. Robb, J. Phys. B **7**, 1006 (1974).
[35]C. Froese-Fischer, Comput. Phys. Commun. **14**, 145 (1978).
[36]L. Liljeby, A. Lindgard, S. Mannervik, E. Veje, and B. Jelenkovic, Phys. Scr. **21**, 805 (1980).
[37]L. A. Collins and B. I. Schneider, Phys. Rev. A **27**, 101 (1983).
[38]T. Sawada, J. E. Purcell, and A. E. S. Green, Phys. Rev. A **4**, 193 (1971).
[39]D. H. Madison and W. N. Shelton, Phys. Rev. A **7**, 499 (1973).
[40]W. C. Stwallay, J. Chem. Phys. **54**, 4517 (1971).
[41]G. D. Meneses, L. E. Machado, G. Csanak, and D. C. Cartwright, J. Phys. B **21**, L717 (1987).
[42]D. H. Madison, G. Csanak, and D. C. Cartwright, J. Phys. B **19**, 3361 (1986).
[43]The wave function for the $M=1$ magnetic level of a (p^5s) electron configuration is the negative of the wave function for the $M=1$ magnetic level of a (ps) electron configuration. See E. U. Condon and H. Obadasi, *Atomic Structure* (Cambridge University Press, Cambridge, 1980), pp. 200 and 201.
[44]J. Kessler, Bull. Am. Phys. Soc. **13**, 98 (1968).